Emission Spectra from NH_3/H_2-Air and $NH_3/H_2/N_2$-Air Spherical Laminar Flames

Yousef M. Almarzooq, Matthew Hay, Mattias A. Turner, Waruna D. Kulatilaka, and Eric L. Petersen
J. Mike Walker '66 Department of Mechanical Engineering, Texas A&M University
College Station, Texas, USA

1 Introduction

Recently, Ammonia (NH_3) has gained attention as a promising, carbon-free, low-cost and safe energy storage option. To predict its combustion behavior in practical systems, the fundamental aspects of its combustion process such as chemical kinetic pathways, flame propagation and stability, and emissions must be understood. This study aimed to improve understanding of NH_3 combustion by exploring emission spectra of spherically expanding flames under controlled lab conditions. Different mixtures of NH_3/H_2-air and $NH_3/H_2/N_2$-air are observed in a range of expanding flames produced in a high-temperature, high-pressure laminar flame speed vessel at Texas A&M University that comes with large windows for optical access. The effect of the equivalence ratio on the NH_3 flame's emission spectra is investigated by varying the equivalence ratio from 0.8 to 1.2. The emission spectra between 200 and 800 nm was investigated, revealing chemiluminescence peaks of OH*, NH*, and NH_2*. The results will be compared to existing data for ammonia flames from the literature. This poster shows the progress of the work on exploring the emissions spectra of spherically expanding flames of NH_3 and its mixtures with H_2 and N_2.

2 Experimental Setup

All experiments were conducted using one of the constant-volume chambers designed for different flame speed measurements at Texas A&M University (TAMU). Two different optical diagnostics were adopted in this study. First, a modified Z-type schlieren imaging setup coupled with a high-speed camera was used to obtain laminar flame speed results. Second, a fiber-coupled spectrometer equipped with an intensified charge-coupled device (ICCD) camera was used to capture the emission spectra of the investigated mixtures. Experiments utilizing the schlieren imaging setup were conducted first. The main reason behind that was to provide a reference frame for every condition (i.e. $\phi = 0.8, 1.0$, and 1.2) where the flame size stays the same. This reference frame was then used to tune the gate delay time on the other optical diagnostic setup (i.e. spectrometer) to ensure that the captured spectra were within the same flame ball for each equivalence ratio, which was about a 9.5-cm flame diameter. A similar experimental setup was utilized by the current research group previously [1]. Detailed descriptions are following.

Correspondence to: yalmarzooq@tamu.edu

A high-temperature, high-pressure (HTHP) vessel having a cylindrical shape was used in the current study. It has an internal diameter of 31.8 cm, a length of 28 cm, and a volume of 25.8 L. This vessel was designed for experiments with initial temperatures and pressures up to 600 K and 30 atm, respectively. Detailed description of this vessel can be found in previous works [2–7]. The HTHP vessel has two, opposed, glass windows with a diameter of 12.7 cm allowing for optical diagnostics of a near-constant pressure spherical flame using the schlieren technique. The spherically propagating flame was captured using a modified Z-type schlieren imaging setup along with a high-speed camera at a rate of 3000 fps. Additionally, a mercury lamp was used on this setup as a light source. The collected images were then processed using an in-house Python code that was designed to capture the flame-front edges. Then, with the help of the non-linear equation examined by Chen [8], the laminar flame speeds were determined. Lastly, the burned-to-unburned density ratios for all experiments were quantified using chemical equilibrium calculations, which then were used to compute the unstretched, unburned flame speed.

Emission spectra of the investigated mixtures were captured using a fiber-coupled spectrometer (Princeton Instruments, model: IsoPlane 160) equipped with an ICCD camera (Princeton Instruments, model: PIMax4). The width of the vertical entrance slit was set to 150 μm. In the current study, the main goal was to obtain preliminary results of the flame spectra for the UV and visible ranges. As a result, a low resolution, with a grating of 300 lines/mm was used to record the data. This grating produces a spectral resolution of 0.204 nm/pixel, approximately. For these lower-resolution tests, the measurable wavelength bandwidth was limited to 200 nm, although the camera/spectrometer setup sensitive to a broader range (i.e. 200 to 850 nm). Therefore, three single-shot experiments were required for every condition to cover the 200-to-800-nm spectral range. These three experiments were distributed at three different locations on the spectrum range, starting at 300 ±100 nm, then 500 ±100, and finally 700 ±100 nm. A calibration of the camera/spectrometer system was done utilizing Princeton Instruments Intellical calibration and a Hg lamp. The signal intensity was not calibrated as the calibration only applies in the visible region. However, the peak emission line at 283 nm was scanned across the pixel array by changing the spectrometers central wavelength position. Scanning the emission line across the pixel array confirmed negligible intensity variation across the pixel array. Taking advantage of the 12.7-cm diameter glass windows on the HTHP vessel, a collimating lens was set at the center of one of the two windows to capture the emission at the desired flame size. Figure 1 shows a schematic of the spectrometer optical setup and test vessel.

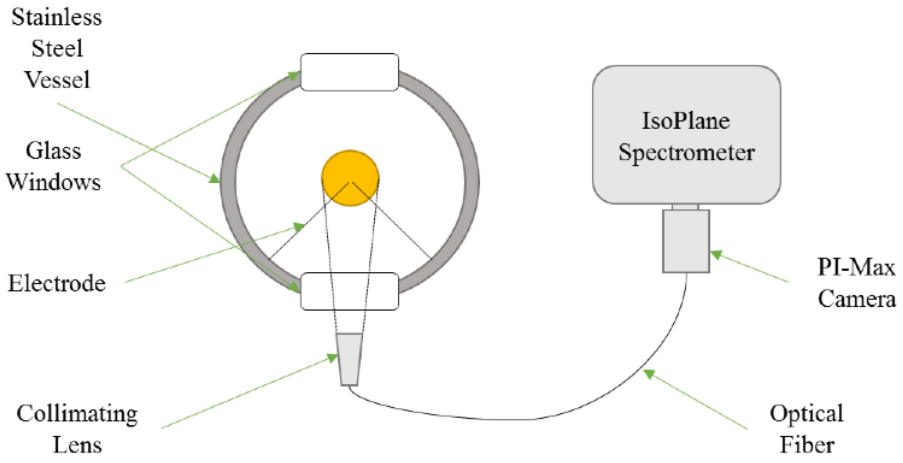

Figure 1: Schematic of the camera/spectrometer system along with the HTHP vessel.

3 Results

Figure 2 presents the emission spectra of (0.4 NH_3 + 0.45 H_2 + 0.15 N_2) / air mixture. Three different equivalence ratios were investigated, namely 0.8, 1.0, and 1.2 over a wavelength range from 200 to 800 nm, covering the UV and visible range. In this figure, all intensities were normalized by the maximum intensity, which in this case the intensity around 717 nm. Not surprisingly, the OH* signal can be seen around 310 nm wavelength for all three equivalence ratios, providing the strongest signal for the stoichiometric case (as expected) compared to the lean and rich ones. Adjacent to the OH* feature, one can see the peak of what most likely is NH*, at approximately 339 nm. Moving toward the visible range, a wide, broadband feature can be seen for all mixtures. Within this broadband, NH_2* was detected at around 610 nm. In addition, at 735 nm a peak was detected and it could be NH_2* or HNO. The NH_2* features captured at 610 nm was becoming stronger as the mixture got richer. The NH* feature captured at 339 nm and the OH* feature at 310 nm were also captured in a previous published study [9]. The experimental apparatus used in [9] was a swirl flame setup, while in the current study a spherically propagating flame apparatus was used. This agreement in detecting different radical species utilizing different experimental apparatus will pave the road towards more advanced chemiluminescence investigation of ammonia flame mixtures adopting the spherically propagating flame apparatus.

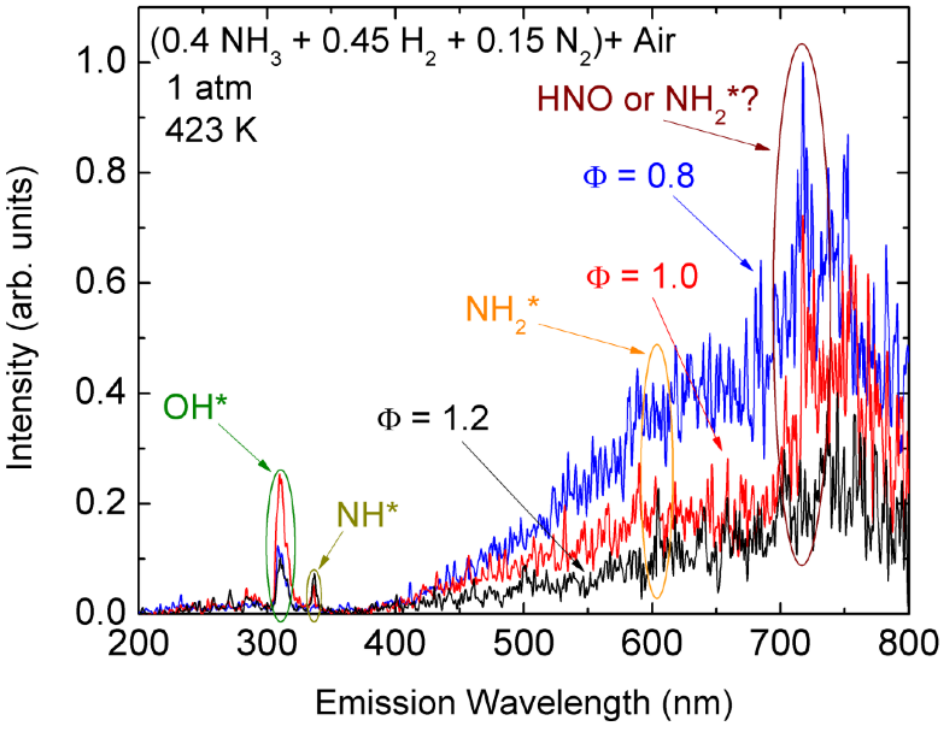

Figure 2: Measured emission spectra of (0.4 NH_3 + 0.45 H_2 + 0.15 N_2) / air at 1 atm, 423 K, and three different equivalence ratios.

References

[1] Turner MA, Parajuli P, Kulatilaka WD, Petersen EL. Emission Spectra of Hydrocarbon Flames Doped with Phosphorus-Containing Compounds. AIAA SCITECH 2022 Forum, American Institute of Aeronautics and Astronautics; n.d. https://doi.org/10.2514/6.2022-0638.

[2] Keesee CL, Guo B, Petersen EL. Proper interpretation and overall accuracy of laminar flame speed measurements of single- and multi-component liquid fuels. Proceedings of the Combustion Institute 2021;38:2225–34. https://doi.org/10.1016/j.proci.2020.06.361.

[3] Keesee CL, Guo B, Petersen EL. Laminar Flame Speed Measurements of Kerosene-Based Fuels Accounting for Uncertainties in Mixture Average Molecular Weight. Journal of Engineering for Gas Turbines and Power 2021;143. https://doi.org/10.1115/1.4049886.

[4] Keesee CL, Guo B, Petersen EL. Laminar Flame Speed Experiments of Alternative Liquid Fuels. Journal of Engineering for Gas Turbines and Power 2019;142. https://doi.org/10.1115/1.4045346.

[5] Krejci MC, Keesee CL, Vissotski AJ, Ravi S, Petersen EL. Effect of Steam Dilution on Laminar Flame Speeds of Syngas Fuel Blends at Elevated Pressures and Temperatures, American Society of Mechanical Engineers Digital Collection; 2019. https://doi.org/10.1115/GT2019-90570.

[6] Krejci MC, Mathieu O, Vissotski AJ, Ravi S, Sikes TG, Petersen EL, et al. Laminar Flame Speed and Ignition Delay Time Data for the Kinetic Modeling of Hydrogen and Syngas Fuel Blends. Journal of Engineering for Gas Turbines and Power 2013;135. https://doi.org/10.1115/1.4007737.

[7] Sikes T, Mathieu O, Kulatilaka WD, Mannan MS, Petersen EL. Laminar flame speeds of DEMP, DMMP, and TEP added to H2- and CH4-air mixtures. Proceedings of the Combustion Institute 2019;37:3775–81. https://doi.org/10.1016/j.proci.2018.05.042.

[8] Chen Z. On the extraction of laminar flame speed and Markstein length from outwardly propagating spherical flames. Combustion and Flame 2011;158:291–300. https://doi.org/10.1016/j.combustflame.2010.09.001.

[9] Mashruk S, Zhu X, Roberts WL, Guiberti TF, Valera-Medina A. Chemiluminescent footprint of premixed ammonia-methane-air swirling flames. Proceedings of the Combustion Institute 2022. https://doi.org/10.1016/j.proci.2022.08.073.